AGU PUBLICATIONS

Geophysical Research Letters

RESEARCH LETTER
10.1002/2014GL061224

**Key Points:**
- Explosive volcanism as recent as < 1 Ga identified on Mercury
- Indicates a 3 Ga history of volcanism, constraining thermal evolution models
- Duration of volcanism on Mercury is similar to that on the Moon

**Supporting Information:**
- Readme
- Table S1
- Figure S1
- Figure S2
- Figure S3
- Figure S4
- Figure S5
- Figure S6
- Figure S7
- Figure S8

**Correspondence to:**
R. J. Thomas,
rebecca.thomas@open.ac.uk

**Citation:**
Thomas, R. J., D. A. Rothery, S. J. Conway, and M. Anand (2014), Long-lived explosive volcanism on Mercury, *Geophys. Res. Lett.*, *41*, 6084–6092, doi:10.1002/2014GL061224.

Received 15 JUL 2014
Accepted 7 AUG 2014
Accepted article online 28 AUG 2014
Published online 4 SEP 2014



# Long-lived explosive volcanism on Mercury

**Rebecca J. Thomas[1], David A. Rothery[1], Susan J. Conway[1], and Mahesh Anand[1,2]**

[1]Department of Physical Sciences, The Open University, Milton Keynes, UK, [2]Department of Earth Sciences, Natural History Museum, London, UK

**Abstract** The duration and timing of volcanic activity on Mercury are key indicators of the thermal evolution of the planet and provide a valuable comparative example for other terrestrial bodies. The majority of effusive volcanism on Mercury appears to have occurred early in the planet's geological history (~4.1–3.55 Ga), but there is also evidence for explosive volcanism. Here we present evidence that explosive volcanism occurred from at least 3.9 Ga until less than a billion years ago and so was substantially more long-lived than large-scale lava plains formation. This indicates that thermal conditions within Mercury have allowed partial melting of silicates through the majority of its geological history and that the overall duration of volcanism on Mercury is similar to that of the Moon despite the different physical structure, geological history, and composition of the two bodies.

## 1. Introduction

In order to constrain models for the composition, internal structure, and formation history of Mercury, it is necessary to assess the duration of volcanism. Model ages obtained for widespread plains-forming lava flows range from ~4.1 to 3.55 Ga [*Denevi et al.*, 2013; *Marchi et al.*, 2013], but little evidence has been found for lava emplacement after that period. It is possible that minor lava flows were emplaced up to 1 Ga [*Prockter et al.*, 2010; *Marchi et al.*, 2011], but this is currently debated [*Chapman et al.*, 2012].

Previous studies [*Head et al.*, 2009; *Kerber et al.*, 2011] identified irregular pits on Mercury with surrounding deposits that are brighter and redder than the planetary average. On the basis of the anomalous spectral characteristics and diffuse margins of these deposits, plus the apparently endogenic nature of the pits, these are widely accepted as pyroclastic deposits formed by explosive volcanism [e.g., *Grott et al.*, 2011; *Byrne et al.*, 2013]. This style of volcanism occurs through separation of volatiles from rising magma, so its occurrence challenges formation models for Mercury predicting a volatile-depleted bulk composition [*Cameron*, 1985; *Fegley and Cameron*, 1987; *Wetherill*, 1988; *Benz et al.*, 2007]. Explosive vents within the Caloris basin clearly superpose the effusively emplaced Caloris interior lava plains [*Head et al.*, 2009; *Rothery et al.*, 2014], and it has been suggested that some explosive volcanism on Mercury in general may have occurred in the Mansurian Period (3.5–1 Ga) [*Goudge et al.*, 2014], which indicates that this type of volcanic activity is a potential indicator of the true duration of volcanic activity.

We use the presence of vents within young, morphologically fresh impact craters and counts of superposed impact craters on pyroclastic deposits to demonstrate a long duration of explosive volcanism on Mercury, extending into the last billion years. We then highlight similarities and differences with the history of volcanic activity on the Moon.

## 2. Methods

### 2.1. Identification of Sites of Explosive Volcanism

We have conducted a global survey for explosive volcanism on Mercury by examining images from the Mercury Dual Imaging System (MDIS) on board NASA's MErcury Surface, Space ENvironment, GEochemistry, and Ranging (MESSENGER) spacecraft. We examined all images at a resolution of 180 m/pixel and better taken prior to 17 March 2013, plus version 9 of the global color and monochrome mosaics at 250 m/pixel produced by the MESSENGER team. In order to identify probable pyroclastic deposits, which are bright and red relative to Mercury's average spectral reflectance [*Kerber et al.*, 2011], we created color composites by placing images taken through the 996, 749, and 433 nm filters of the Wide Angle Camera (WAC) in the red, green, and blue bands, respectively.

**Table 1.** Locations and Crater Retention Model Ages for Pyroclastic Deposits on Mercury

| | | | Pyroclastic Deposit Ages (Ga) | |
|---|---|---|---|---|
| Description | Longitude (°E) | Latitude (°N) | NPF | MPF |
| Annular pit (AP2) | −135.5 | −8.4 | 3.9 (+0.0/−0.1) 3.6 (+0.1/−0.1) | 3.7 (+0.0/−0.0) |
| NE Rachmaninoff | 64.1 | 36.1 | 3.7 (+0.0/−0.0) | |
| Picasso crater | 50.8 | 3.9 | 3.4 (+0.0/−0.1) | |
| RS-03 (within Caloris) | 146.2 | 22.4 | 3.4 (+0.1/−0.1) | |
| N Rachmaninoff | 57.4 | 36.0 | 3.3 (+0.1/−0.2) | |

This survey led to the identification of 150 locations where the association of irregular pits and relatively bright, red deposits indicates explosive volcanic activity (Figure S1), a considerable advance on the number of such locations previously documented [*Kerber et al.*, 2011; *Goudge et al.*, 2014]. The majority (79%) of these are within impact craters. This provides a means of constraining the maximum age of the volcanism in each case, as these pits must post-date their host crater and any cross-cut intra-crater fills.

### 2.2. Assessing the Ages of Craters Hosting Explosive Volcanism

Impact craters degrade over time as a result of subsequent impacts and the resulting regolith-forming processes, and hence the degree of degradation of the crater indicates its age [*Spudis and Guest*, 1988]. This provides an essential tool for assessing the maximum age of pyroclastic deposits that overlie the impact crater. Where a pyroclastic deposit is small and thin (tens of $km^2$ and a few m thick), it is a poor candidate for dating by counting superposed impact craters, because it does not obscure underlying older craters and extends over an area smaller than desirable for the counting method at the resolution of the images available. Therefore, establishing the age of an impact crater in which a vent or pyroclastic deposit occurs is the most robust method of determining a maximum age for the volcanic activity.

Where vents and pyroclastic deposits occur within an impact crater or on its proximal ejecta, we have estimated the age of the host crater on the basis of its state of degradation. We use the scheme outlined by *Barnouin et al.* [2012] for Mercury (following *Spudis and Guest* [1988]), which assigns a crater a degradation state on the basis of attributes such as the preservation of its ejecta blanket, presence of superposed craters, and modification of its terraces.

### 2.3. Dating Pyroclastic Deposits

As discussed above, dating small-scale pyroclastic deposits on the basis of superposed impact craters is problematic. However, where deposits are thick and large (hundreds of $km^2$ and tens of m thick) it may be possible to determine their age using this method. We identified such deposits at five locations (Table 1) and counted superposed impact craters on the deposits and other surfaces in their vicinity using CraterTools in ArcGIS [*Kneissl et al.*, 2011]. We recorded fractional counts where a crater intersects the counting area boundary to avoid overestimation of large craters straddling that boundary. We compared the crater size-frequency distribution to the established production and chronology function of *Neukum et al.* [2001] to derive model ages for the formation of these surfaces. We also explored the effect of using a different crater production function to assess the surface age by comparing these model ages with those indicated by the Model Production Function (MPF) of *Marchi et al.* [2009] at one location.

We excluded craters from the analysis if we judged them to be secondaries on the basis of a chained or clustered arrangement or a non-circular shape. After removal of this fraction of the population, we performed a randomness analysis [*Michael et al.*, 2012] to statistically assess the degree to which the remaining craters are clustered. Because secondary impact craters are not always distinguishable on the basis of clustering, and because of the high proportion of secondary craters on Mercury [*Strom et al.*, 2008], it is probable that we have not been able to exclude all secondaries. These will affect the model ages derived using the two production functions to different degrees. The Neukum Production Function (NPF) is a modification of the lunar production function, taking into account differences in the velocity of impactors and impact rate at Mercury versus the Moon [*Neukum et al.*, 2001]. As the density of secondaries is thought to differ on Mercury and the Moon [*Strom et al.*, 2011; *Xiao et al.*, 2014], the NPF may not adequately account for non-obvious secondaries in its model age estimate, and because secondaries are spatially non-random, this may lead to an artificially high or low age estimate. On the other hand, the MPF is constructed by determining the crater

population expected from the population of impactors at Mercury and then calibrating that to the lunar production function [*Marchi et al.*, 2009]. It does not explicitly include secondaries, so if they are present in the counted population, they will lead to an overestimate of surface age. However, the presence of a large population of secondaries would alter the shape of the crater density plot versus that expected for Mercury. If plots lie along established Mercury isochrons, this is a good indication that secondaries do not dominate the counted population.

We are aware that a pyroclastic deposit, even though sufficiently thick to produce the characteristic "red" surface color, might be too thin to hide the underlying craters. Therefore, where suitable images were available we produced stereo-derived digital elevation models (DEMs) of the pit and deposit using the Ames Stereo Pipeline (ASP) [*Moratto et al.*, 2010]. Where the deposit lies on a surface that may reasonably be expected to have been originally flat, anomalous relief around the pit is potentially attributable to pyroclastic deposition. To calculate the maximum rim height of an older crater that would have been erased by a deposit observed in the DEM, we used *Pike*'s [1988] equation for bowl-shaped craters on Mercury:

$$h = 0.052D^{0.930} \quad (1)$$

where $h$ = deposit thickness and $D$ = crater diameter. If the maximum crater diameter upon which our model age determinations were based is less than $D$, it is reasonable to state that the pyroclastic deposit is the surface being dated. Where topography was not available, we tested whether the model ages we derived dated the pyroclastic deposits or the background surface by also dating a surface at a distance from the pit and comparing this with the model age near the pit. If fewer craters per unit area superpose the pyroclastic deposit than the surface remote from the pit, either the pyroclastic deposit is significantly younger or its physical properties led to more rapid degradation of superposed craters.

## 3. Results

### 3.1. Evidence for Recent Explosive Volcanism

In the supporting information, we catalogue and illustrate the global distribution of all 150 groups of volcanic pits with associated bright, red deposits that we have identified on Mercury (Table S1 and Figure S1). Of the 118 that occur within impact craters, the majority are within moderately degraded craters dating to the Calorian Period (3.9–3.5 Ga), but 28 are in only slightly degraded craters dating to the Mansurian Period (3.5–1 Ga) and four are in very fresh craters with bright ejecta that date to the late Mansurian ($<$c.1.7 Ga) or Kuiperian ($<$1 Ga) Period (using the criteria of *Spudis and Guest* [1988]). The age of the host crater provides a maximum age for the pyroclastic activity in each instance. Here we present two examples that provide the clearest evidence of recent (i.e., late Mansurian to Kuiperian) explosive volcanism on Mercury.

The first example is within a 21 km diameter crater at 67.9° W, 8.4° N (Figure 1). Explosive volcanic activity at this location is evident in the form of a large pit cutting the northern rim of the impact crater (white arrow, Figure 1b), as well as a relatively red deposit that is bright to a radius of 19 km around the largest pit, and fainter to a radius of 26 km. The deposit is centered on the pit, not on the crater, from which we conclude that it was sourced from the pit rather than exhumed during formation of the impact crater. The crisp rim and undegraded ejecta blanket show that the host crater is relatively young and probably formed in the late Mansurian. Though its floor is superposed by numerous small impact craters, which would usually indicate a long duration of exposure, the color image (Figure 1a) reveals that these are part of a bright ray of secondary craters from the Hokusai impact to the northeast. The host crater therefore predates Hokusai, which is of Kuiperian age on the basis of its well-preserved bright rays [*Spudis and Guest*, 1988]. The size and density of impact craters superposed on those parts of the ejecta blanket that appear relatively unaffected by Hokusai secondaries are low, supporting a young age (Figure 1c). Because of the small sampling area and uncertainties introduced by the higher proportion of secondaries at small crater diameters, we are cautious about ascribing an age to this impact crater on the basis of crater counting. However, the model age arrived at using the NPF, 1.7 Ga ± 0.3 (Figure 1d), is consistent with the fresh morphology of the crater.

In the second example, the pit cuts the wall terraces within Kuniyoshi, a 26 km diameter crater at 37.4° W, 57.8° S (Figure 2). This crater's peak and walls have a crisp appearance, and its ejecta blanket is undegraded and has a high albedo. Such a fresh morphology characterizes Kuiperian-aged ($<$1 Ga) impact craters. Another important characteristic of Kuiperian-aged craters is the presence of rays. It is unclear whether

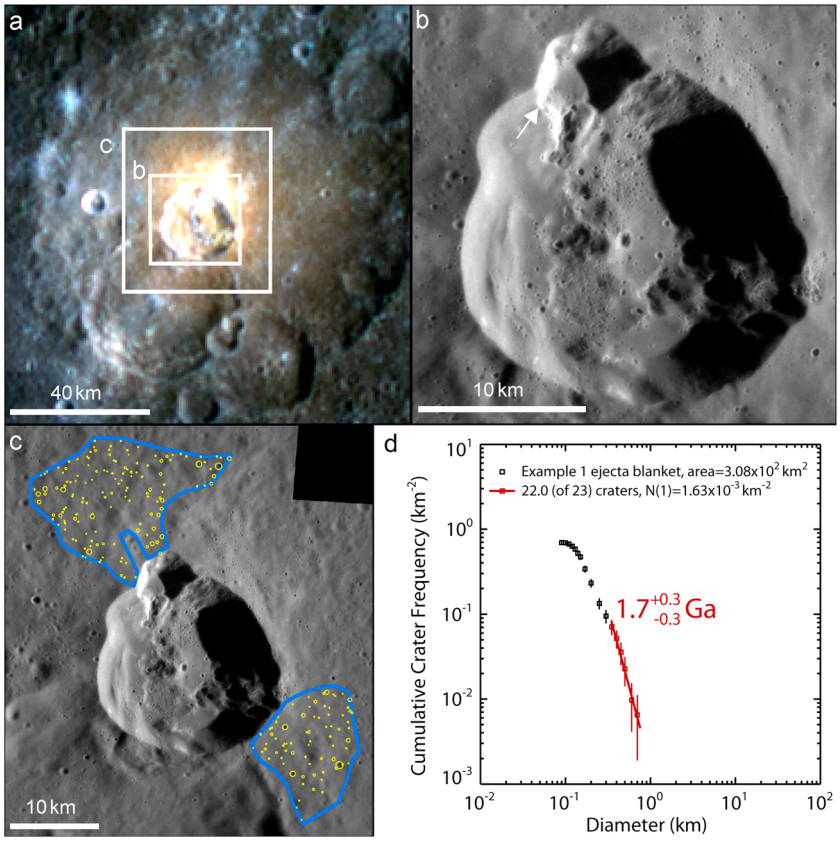


**Figure 1.** A small, fresh late Mansurian crater with associated relatively bright and red deposits (67.9° W, 8.4° N). (a) Color composite showing a surrounding spectral anomaly centered at the northern rim of the crater and superposition by a bright ray from Hokusai crater to the northeast. (Images EW0241501576I, EW0241501568G, and EW0241501572F, with panchromatic sharpening using image EW0223917664G); (b) higher-resolution monochrome image with white arrow indicating a large pit in the northern rim of the crater (image EN0239206510M); (c) areas sampled to derive model ages through crater counting outlined in blue, superposed impact craters: yellow circles (image EN0239206510M and EN0239206492M); (d) crater size-frequency distribution within the counting areas outlined in (c) indicating a maximum age for volcanic activity of ~1.7 Ga. (Image credit: NASA/Johns Hopkins University Applied Physics Laboratory/Carnegie Institution of Washington.)

these are present, but bright material surrounds the crater and there is a suggestion of alignments radial to the crater within this (Figure 2a). A slightly smaller crater 200 km northwest of Kuniyoshi crater has radial alignments that appear to be rays, and yet its morphology is less crisp than, or at most as fresh as, that of Kuniyoshi (Figure 2c). Its rays reach a distance from the crater that is less than the radius of the high-albedo material surrounding Kuniyoshi, so if present to that distance around Kuniyoshi, rays would not be visible against the bright material. A young age for Kuniyoshi is supported by the very low density of impact craters superposed on its ejecta blanket: only 15 craters, all $<1$ km diameter, are visible over an area 1581 km$^2$ (Figure 2b). Their morphology suggests that six of these are secondaries (red in Figure 2b) and given the high proportion of secondaries in the small crater population of Mercury relative to other planets, it is probable several of the remaining craters are as well. On the basis of this sparsity of superposed craters, the freshness of the host crater's morphology, and the possible presence of rays, we date this crater to the Kuiperian, most probably to its earliest part. Two pits a few kilometers apart incise the crater's northern terraces and rim, and are surrounded by a relatively bright and red deposit. These indicate that explosive volcanism occurred here after the crater's formation, and hence in the Kuiperian Period.

Interestingly, this crater lies adjacent to a 410 km long region with numerous pits crosscutting and bright deposits overlying, Tolstojan- (4.0–3.9 Ga [*Spudis and Guest*, 1988]) to Mansurian-age impact craters (Figure 2a). The morphology of these pits is not appreciably more subdued than those within Kuniyoshi (Figure 2d), so explosive activity in this entire region may have been equally recent.

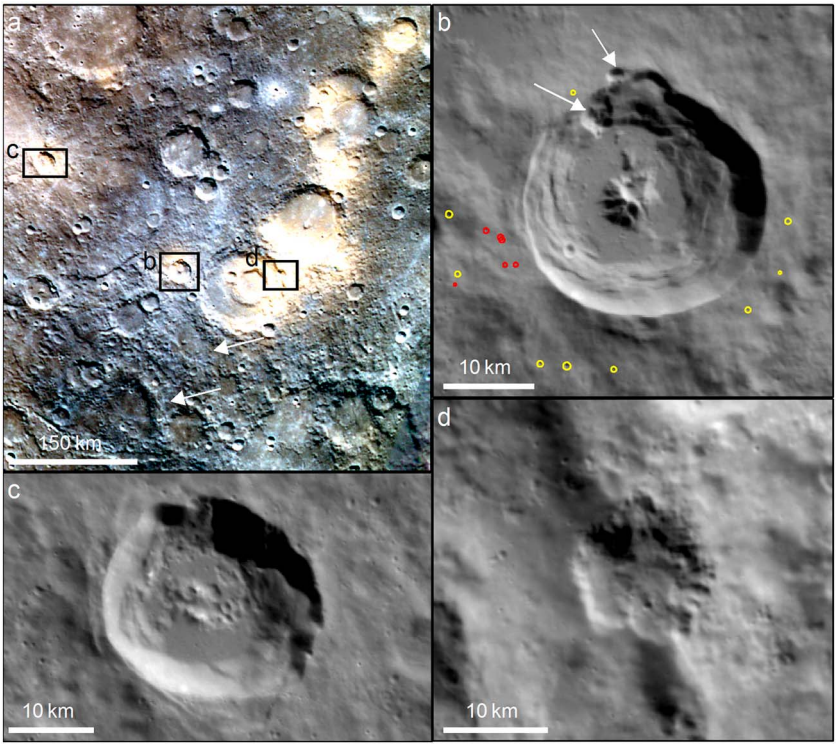


**Figure 2.** Explosive volcanism at Kuniyoshi, a young (Kuiperian), fresh crater at 37.4° W, 57.8° S. (a) Color composite image showing bright, red deposits at the northern rim of Kuniyoshi (located within box b) and a linear region with multiple centers of relatively bright and red deposits to its east and northeast, all indicative of explosive volcanism. White arrows: possible rays from Kuniyoshi, black rectangles: extents of b, c, and d. (Images EW1005108006I, EW1005108026G, and EW1005108010F); (b) monochrome image showing Kuniyoshi's crisp morphology and undegraded ejecta blanket and endogenic pits in its north wall (white arrows). Primary impact craters on its ejecta blanket circled in yellow; secondary impact craters circled in red (Image EN0239251642M); (c) a crater to the northwest of Kuniyoshi: its morphology is not as crisp as that of Kuniyoshi, but it appears to have visible rays in (a). (Image EN0239124609M); (d) vent with crisp morphology in a crater to the east of Kuniyoshi. (Image credit: NASA/Johns Hopkins University Applied Physics Laboratory/Carnegie Institution of Washington.)

The above evidence indicates that explosive volcanic activity occurred on Mercury until the Kuiperian. While the evidence for a young age is most conclusive at these two locations, they are not unique: pyroclastic deposits occur in other young craters and the morphology of the associated pits in some older craters is distinctly more crisp than that of the host crater, indicating a considerably younger but, as yet, unquantifiable age. The freshest (least degraded) internal vent morphology yet documented is inside the four youngest vents within the RS-03 compound vent in the southwest of the Caloris basin [*Rothery et al.*, 2014].

### 3.2. Evidence for the Duration of Explosive Volcanic Activity

Additionally, we have found evidence for explosive volcanism as early as the Calorian Period (3.9–3.5 Ga). At five locations where pyroclastic deposits were sufficiently thick to be good candidates for dating in this way, we obtained model ages from 3.9 (±0.1) to 3.3 Ga (+0.1/−0.2) (Table 1). Below we present the evidence for the oldest and youngest of these ages in further detail.

#### 3.2.1. Pit Annular to a Crater Central Peak (AP2)

At this location an endogenic pit (which apparently acted as a volcanic vent) has formed around the central structure of a very old, degraded impact crater (Figure S2). This pit is surrounded by deposits with the relatively bright and red spectrum characteristic of Mercury's pyroclastic deposits.

Fitting an NPF isochron to the cumulative density plot of 1.2 to 2 km diameter craters around the pit gives a model age of 3.9 Ga (+0.0/−0.1) (Figure S3a). We interpret this as the age of the pyroclastic deposit rather than of the floor of the crater because the pyroclastic deposit appears to be up to 360 m thick here (Figure S4). This is sufficiently thick to erase the record of craters in the 1.2–2 km range. Fitting craters of all diameters to

the MPF with a main belt asteroid (MBA) flux and modeling the impacted surface as a cohesive soil with a strength of $1 \times 10^6$ dyne/cm$^2$, gives a model age of 3.7 Ga (±0.0) (Figure S3b). Because a resurfacing correction [*Michael and Neukum*, 2010] cannot be applied to the MPF, this fit includes a single large crater at the outer margin of the deposit. This crater may have formed prior to the pyroclastic activity, in which case its inclusion will have inflated the MPF age. We have obtained very similar model ages for a smooth effusive volcanic plain 140 km to the east: a NPF model age of 3.8 Ga (±0.0) and a MPF model age of 3.6 Ga (±0.0) (using a cohesive soil scaling law, MBA-like flux, and a strength of $1 \times 10^6$ dyne/cm$^2$) (Figure S3). Thus, although the MPF gives a younger model age than the NPF, as noted elsewhere [*Massironi et al.*, 2009], both indicate that explosive volcanism was approximately contemporaneous with large-scale effusive volcanism in this region. An underabundance of smaller craters (<1.15 km diameter) causes a step in the cumulative crater density curve at small crater sizes, which may indicate more recent deposition of a thinner deposit [*Michael and Neukum*, 2010]. This younger population of superposed craters is also apparent in a differential plot (Figure S5). This resurfacing event has a NPF model age of 3.6 Ga (±0.1), and the size range of the craters affected indicates the younger layer is 59–62 m thick.

#### 3.2.2. North of Rachmaninoff Basin (N Rachmaninoff)

This is a large (~33 km radius) pit 360 km north of the center of the Rachmaninoff impact basin (Figure S6). The pit has an irregular outline and lacks an ejecta blanket or terraces, so we regard it as endogenic. It is surrounded by a deposit that clearly overlies impact craters on the continuous ejecta blanket of the Rachmaninoff basin (white arrows in Figure S6c), indicating that it post-dates Rachmaninoff. The deposit is thick to the south and west of the pit, obscuring the walls and floors of large craters, but appears thinner to the north of the pit (Figure S8). We interpret the deposit as pyroclastic on the basis of its association with the pit, the bright and red spectral signature of the surface, and the diffuse margins of the overall spectral anomaly. The high relief in the south and west suggests deposition by flow here. In the absence of a nearby impact crater that could have generated this material by impact melting (Figure S6b), we suggest that this was clastogenic flow resulting from a high-flux pyroclastic eruption. The cumulative density of larger craters (1.2–2 km diameter) in the circum-pit area indicates a NPF model age of 3.6 Ga (±0.1), and a step in the cumulative plot at smaller crater sizes (0.6–1.1 km) suggests resurfacing dating to 3.3 Ga (+0.1/−0.2) by a layer of 57–62 m thick (Figure S7). Because the larger craters occur in the north and east, where the deposits appear thinner, it is probable that the density of large craters indicates the model age of the underlying surface, whereas the model age of 3.3 Ga dates the pyroclastic activity.

The evidence above demonstrates that thick, large-scale pyroclastic deposits were deposited on Mercury during and up to ~400 million years after the period of widespread plains-forming effusive volcanism. The evidence for two periods of activity at AP2 is consistent with earlier work [*Rothery et al.*, 2014], showing that explosive volcanic vents on Mercury can have a prolonged eruptive history.

## 4. Discussion

Our results indicate a long history of volcanism on Mercury, with effusive volcanism from ~4.1 Ga [*Marchi et al.*, 2013] and explosive volcanism continuing until as little as a billion years ago. This reinforces the necessity of incorporating long-lived volcanism into models of the thermo-chemical evolution of the planet [e.g., *Grott et al.*, 2011; *Michel et al.*, 2013; *Tosi et al.*, 2013], even if the age of possible young lava deposits [*Prockter et al.*, 2010] is revised upward. Because dating craters that predate pyroclastic vents and deposits gives only a maximum age for the volcanic activity, our results do not allow us to calculate the volume of late-stage explosive volcanism. However, we do find that pyroclastic activity continued until long after the period when voluminous lava eruption formed expansive volcanic plains. In addition to reflecting a decrease in melt production due to secular cooling, it is probable that this change in eruptive style was favored by changes in the crust through time, e.g., due to the development of compressional stress, as indicated by pervasive fault-related landforms across the planet that date from shortly after 3.8 Ga [*Strom et al.*, 1975; *Watters et al.*, 2012], and thickening of the lithosphere due to planetary cooling. Both these conditions would impede magma ascent. Slow magma ascent allows exsolution of dissolved volatiles and coalescence of bubbles before eruption, promoting intermittent explosive strombolian eruption [*Wilson and Head*, 1981]. Further, if magma rise is so inhibited that a dike stalls below the surface, a magma chamber may form. Here, crystallization can lead to volatile oversaturation in the remaining melt [*Tait et al.*, 1989; *Parfitt et al.*, 1993],

and these volatiles can exsolve in the low-pressure, near-surface environment. The resultant overpressure can trigger the propagation of dikes to the surface in an explosive eruption [*Head et al.*, 2002], particularly if, as is the case under impact craters on Mercury (R. J. Thomas et al., Mechanisms of explosive volcanism on Mercury: Implications from its global distribution and morphology, submitted to *Journal of Geophysical Research*, 2014), there are preexisting fractures in the overlying crust. Thus, it is to be expected that as magma ascent became impeded late in the planet's history, the volatile content in erupting magmas became elevated and the eruptions more explosive.

A further implication of our findings is that the longevity of volcanism on Mercury is similar to that on the Moon, but that the style of late volcanism differed on the two planets. On the Moon, lava surfaces have been dated to 1.2 Ga [*Hiesinger*, 2003] or even to 0.8 Ga [*Huang et al.*, 2011]. Pyroclastic deposits have proved difficult to date by crater-counting because their unconsolidated nature leads to rapid degradation of small superposed impact craters [*Lucchitta and Sanchez*, 1975]. However, stratigraphic relationships in most cases indicate a maximum Late Imbrian (3.2 to 3.7 Ga) age [e.g., *Head and Wilson*, 1979; *Hiesinger et al.*, 2000; *Whitford-Stark and Head*, 2000] and young ($<$1 Ga) explosive volcanism has only been proposed at one location on this basis [*Spudis*, 1989]. Conversely, although we have shown that pyroclastic activity was very long-lived on Mercury, late effusive volcanism is as yet unproved. A young (~1 Ga) age proposed for smooth plains within Rachmaninoff basin [*Prockter et al.*, 2010] is currently being revised on the basis of the higher number of craters visible in higher resolution images [*Chapman et al.*, 2012] and no other lava surface has been dated to younger than 3.55 Ga.

Late effusive volcanism on the Moon is thought to have been enabled both by a concentration of heat-producing elements in the western nearside lunar crust [*Jolliff et al.*, 2000] and by extension at the margins of large impact basins due to flexural loading [*Head and Wilson*, 1992; *McGovern and Litherland*, 2011]. As the loading is a result of the accumulation of thick, dense lavas in basins because the low density of the lunar primary crust prevented eruption in other regions with higher elevations and a greater crustal thickness, both of these factors are a result of compositional variations in the Moon's crust. Mercury's crust does not appear to have such extreme spatial variations in composition [*Nittler et al.*, 2011], so neither the stress-regime nor crustal heating would be expected to facilitate effusive volcanism to such a degree on Mercury late in its history. If the two bodies had a similar duration of volcanism despite their different composition, internal structure and geological history, this may indicate that similar mechanisms, such as insulation by a megaregolith [*Ziethe et al.*, 2009; *Grott et al.*, 2011], allowed a long duration of magma production, but that differing physical conditions in their respective crusts led to differing styles of late volcanism.

Compositional differences in the magma may also have led to greater explosivity on Mercury. In particular, it is possible that Mercury's magma had a higher volatile content than lunar magma. This would explain the large size of pyroclastic deposits on Mercury relative to those on the Moon [*Kerber et al.*, 2011] even without concentration of volatiles at shallow depths before eruption. Lacking, as we do, samples of the products of Hermean volcanism, this possibility is difficult to assess. However, future spectral analyses using data gathered by MESSENGER and the forthcoming BepiColombo mission [*Benkhoff et al.*, 2010] may lead to valuable insights into the composition of both effusive and pyroclastic deposits on Mercury.

**Acknowledgments**

The image data used for the results of this paper are available at the PDS Geosciences Node of Washington University, St. Louis, USA. All other data are either within the supporting information or available from the authors on request. Rebecca Thomas acknowledges a PhD studentship from the Science and Technology Facilities Council (UK) (ST/K502212/1). David Rothery acknowledges support from UKSA PP/E002412/1 and ST/M002101/1, and STFC ST/L000776/1. We thank Simone Marchi of the Solar System Exploration Research Virtual Institute, Southwest Research Institute, Boulder, CO for his invaluable help in producing model production function ages for this paper and Christian Klimczak, Thomas Platz and Paul Byrne for their helpful reviews.

The Editor thanks T. Platz, Paul Byrne, and Christian Klimczak for their assistance in evaluating this paper.

## References

Barnouin, O. S., M. T. Zuber, D. E. Smith, G. A. Neumann, R. R. Herrick, J. E. Chappelow, S. L. Murchie, and L. M. Prockter (2012), The morphology of craters on Mercury: Results from MESSENGER flybys, *Icarus*, *219*(1), 414–427, doi:10.1016/j.icarus.2012.02.029.

Benkhoff, J., J. van Casteren, H. Hayakawa, M. Fujimoto, H. Laakso, M. Novara, P. Ferri, H. R. Middleton, and R. Ziethe (2010), BepiColombo—Comprehensive exploration of Mercury: Mission overview and science goals, *Planet. Space Sci.*, *58*(1–2), 2–20, doi:10.1016/j.pss.2009.09.020.

Benz, W., A. Anic, J. Horner, and J. A. Whitby (2007), The origin of Mercury, *Space Sci. Rev.*, *132*(2–4), 189–202, doi:10.1007/s11214-007-9284-1.

Byrne, P. K., C. Klimczak, D. A. Williams, D. M. Hurwitz, S. C. Solomon, J. W. Head, F. Preusker, and J. Oberst (2013), An assemblage of lava flow features on Mercury, *J. Geophys. Res. Planets*, *118*, 1303–1322, doi:10.1002/jgre.20052.

Cameron, A. G. W. (1985), The partial volatilization of Mercury, *Icarus*, *64*(2), 285–294, doi:10.1016/0019-1035(85)90204-0.

Chapman, C. R., W. J. Merline, S. Marchi, L. M. Prockter, C. I. Fassett, J. W. Head, S. C. Solomon, and Z. Xiao (2012), The young inner plains of Mercury's Rachmaninoff basin reconsidered, paper presented at 43rd Lunar Planet. Sci. Conf., abstract 1607. [Available at http://www.lpi.usra.edu/meetings/lpsc2012/pdf/1607.pdf.]

Denevi, B. W., et al. (2013), The distribution and origin of smooth plains on Mercury, *J. Geophys. Res. Planets*, *118*, 891–907, doi:10.1002/jgre.20075.

Fegley, B., and A. G. W. Cameron (1987), A vaporization model for iron/silicate fractionation in the Mercury protoplanet, *Earth Planet. Sci. Lett.*, *82*, 207–222.

Goudge, T. A., et al. (2014), Global inventory and characterization of pyroclastic deposits on Mercury: New insights into pyroclastic activity from MESSENGER orbital data, *J. Geophys. Res. Planets*, *119*, 635–658, doi:10.1002/2013JE004480.

Grott, M., D. Breuer, and M. Laneuville (2011), Thermo-chemical evolution and global contraction of mercury, *Earth Planet. Sci. Lett.*, *307*(1–2), 135–146, doi:10.1016/j.epsl.2011.04.040.

Head, J. W., and L. Wilson (1979), Alphonsus-type dark-halo craters: Morphology, morphometry and eruption conditions, *Lunar Planet. Sci. Conf. Proc.*, *10*, 2861–2897.

Head, J. W., and L. Wilson (1992), Lunar mare volcanism: Stratigraphy, eruption conditions, and the evolution of secondary crusts, *Geochim. Cosmochim. Acta*, *56*, 2155–2175.

Head, J. W., L. Wilson, and C. M. Weitz (2002), Dark ring in southwestern Orientale Basin: Origin as a single pyroclastic eruption, *J. Geophys. Res.*, *107*(E1), 5001, doi:10.1029/2000JE001438.

Head, J. W., et al. (2009), Volcanism on Mercury: Evidence from the first MESSENGER flyby for extrusive and explosive activity and the volcanic origin of plains, *Earth Planet. Sci. Lett.*, *285*(3–4), 227–242, doi:10.1016/j.epsl.2009.03.007.

Hiesinger, H., R. Jaumann, G. Neukum, and J. W. Head (2000), Ages of mare basalts on the lunar nearside, *J. Geophys. Res.*, *105*(E12), 29,239–29,275, doi:10.1029/2000JE001244.

Hiesinger, H. (2003), Ages and stratigraphy of mare basalts in Oceanus Procellarum, Mare Nubium, Mare Cognitum, and Mare Insularum, *J. Geophys. Res.*, *108*(E7), 5065, doi:10.1029/2002JE001985.

Huang, J., L. Xiao, X. He, L. Qiao, J. Zhao, and H. Li. (2011), Geological characteristics and model ages of Marius Hills on the Moon, *J. Earth Sci.*, *22*, 601–609.

Jolliff, B. L., J. J. Gillis, L. A. Haskin, R. L. Korotev, and M. A. Wieczorek (2000), Major lunar crustal terranes: Surface expression and crust-mantle origins, *J. Geophys. Res.*, *105*(E2), 4197–4216, doi:10.1029/1999JE001103.

Kerber, L., J. W. Head, D. T. Blewett, S. C. Solomon, L. Wilson, S. L. Murchie, M. S. Robinson, B. W. Denevi, and D. L. Domingue (2011), The global distribution of pyroclastic deposits on Mercury: The view from MESSENGER flybys 1–3, *Planet. Space Sci.*, *59*(15), 1895–1909, doi:10.1016/j.pss.2011.03.020.

Kneissl, T., S. van Gasselt, and G. Neukum (2011), Map-projection-independent crater size-frequency determination in GIS environments - New software tool for ArcGIS, *Planet. Space Sci.*, *59*(11–12), 1243–1254, doi:10.1016/j.pss.2010.03.015.

Lucchitta, B. K., and A. G. Sanchez (1975), Crater studies in the Apollo 17 region, *Lunar Planet. Sci. Conf. Proc.*, *6*, 2427–2441.

Marchi, S., S. Mottola, G. Cremonese, M. Massironi, and E. Martellato (2009), A new chronology for the Moon and Mercury, *Astron. J.*, *137*(6), 4936–4948, doi:10.1088/0004-6256/137/6/4936.

Marchi, S., M. Massironi, G. Cremonese, E. Martellato, L. Giacomini, and L. Prockter (2011), The effects of the target material properties and layering on the crater chronology: The case of Raditladi and Rachmaninoff basins on Mercury, *Planet. Space Sci.*, *59*(15), 1968–1980, doi:10.1016/j.pss.2011.06.007.

Marchi, S., C. R. Chapman, C. I. Fassett, J. W. Head, W. F. Bottke, and R. G. Strom (2013), Global resurfacing of Mercury 4.0–4.1 billion years ago by heavy bombardment and volcanism, *Nature*, *499*(7456), 59–61, doi:10.1038/nature12280.

Massironi, M., G. Cremonese, S. Marchi, E. Martellato, S. Mottola, and R. J. Wagner (2009), Mercury's geochronology revised by applying Model Production Function to Mariner 10 data: Geological implications, *Geophys. Res. Lett.*, *36*, L21204, doi:10.1029/2009GL040353.

McGovern, P. J., and M. M. Litherland (2011), Lithospheric stress and basaltic magma ascent on the Moon, with implications for large volcanic provinces and edifices, presented at 42nd Lunar Planet. Sci. Conf., abstract 2587, doi:10.1038/NGEO897.

Michael, G. G., and G. Neukum (2010), Planetary surface dating from crater size – Frequency distribution measurements: Partial resurfacing events and statistical age uncertainty, *Earth Planet. Sci. Lett.*, *294*(3–4), 223–229, doi:10.1016/j.epsl.2009.12.041.

Michael, G. G., T. Platz, T. Kneissl, and N. Schmedemann (2012), Planetary surface dating from crater size–frequency distribution measurements: Spatial randomness and clustering, *Icarus*, *218*(1), 169–177, doi:10.1016/j.icarus.2011.11.033.

Michel, N. C., S. A. Hauck, S. C. Solomon, R. J. Phillips, J. H. Roberts, and M. T. Zuber (2013), Thermal evolution of Mercury as constrained by MESSENGER observations, *J. Geophys. Res. Planets*, *118*, 1033–1044, doi:10.1002/jgre.20049.

Moratto, S. Z. M., M. J. Broxton, R. A. Beyer, M. Lundy, and K. Husmann (2010), Ames Stereo Pipeline, NASA's Open Source Automated Stereogrammetry, presented at 41st Lunar Planet. Sci. Conf., abstract 2364. [Available at http://www.lpi.usra.edu/meetings/lpsc2010/pdf/2364.pdf.]

Neukum, G., J. Oberst, H. Ho, R. Wagner, and B. A. Ivanov (2001), Geologic evolution and cratering history of Mercury, *Planet. Space Sci.*, *49*, 1507–1521.

Nittler, L. R., et al. (2011), The major-element composition of Mercury's surface from MESSENGER X-ray spectrometry, *Science*, *333*(6051), 1847–50, doi:10.1126/science.1211567.

Parfitt, E. A., L. Wilson, and J. W. Head (1993), Basaltic magma reservoirs: Factors controlling their rupture characteristics and evolution, *J. Volcanol. Geotherm. Res.*, *55*(1–2), 1–14, doi:10.1016/0377-0273(93)90086-7.

Pike, R. J. (1988), Geomorphology of impact craters on Mercury, in *Mercury*, edited by F. Vilas, C. R. Chapman, and M. S. Matthews, pp. 165–273, Univ. of Ariz. Press, Tucson, Ariz.

Prockter, L. M., et al. (2010), Evidence for young volcanism on Mercury from the third MESSENGER flyby, *Science*, *329*(5992), 668–671, doi:10.1126/science.1188186.

Rothery, D. A., R. J. Thomas, and L. Kerber (2014), Prolonged eruptive history of a compound volcano on Mercury: Volcanic and tectonic implications, *Earth Planet. Sci. Lett.*, *385*, 59–67.

Spudis, P. D. (1989), Young dark mantle deposits on the Moon, in *Workshop on Lunar Volcanic Glasses: Scientific and Resource Potential. A Lunar and Planetary Institute Workshop, Sponsored by LPI and the Lunar and Planetary Sample Team, Held October 10–11, 1989, at the Lunar and Planetary Institute, in Houston, Texas*, edited by J. W. Delano and G. H. Heiken, 60 pp., Lunar and Planetary Institute, Houston, Tex.

Spudis, P. D., and J. E. Guest (1988), Stratigraphy and geologic history of Mercury, in *Mercury*, edited by F. Vilas, C. R. Chapman, and M. S. Matthews, pp. 118–164, Univ. of Ariz. Press, Tucson, Ariz.

Strom, R. G., N. J. Trask, and J. E. Guest (1975), Tectonism and volcanism on Mercury, *J. Geophys. Res.*, *80*(17), 2478–2507, doi:10.1029/JB080i017p02478.

Strom, R. G., C. R. Chapman, W. J. Merline, S. C. Solomon, and J. W. Head (2008), Mercury cratering record viewed from MESSENGER's first flyby, *Science*, *321*(5885), 79–81, doi:10.1126/science.1159317.

Strom, R. G., M. E. Banks, C. R. Chapman, C. I. Fassett, J. A. Forde, J. W. Head, W. J. Merline, L. M. Prockter, and S. C. Solomon (2011), Mercury crater statistics from MESSENGER flybys: Implications for stratigraphy and resurfacing history, *Planet. Space Sci.*, *59*(15), 1960–1967, doi:10.1016/j.pss.2011.03.018.

Tait, S., C. Jaupart, and S. Vergniolle (1989), Pressure, gas content and eruption periodicity of a shallow, crystallising magma chamber, *Earth Planet. Sci. Lett.*, *92*, 107–123.

Tosi, N., M. Grott, A.-C. Plesa, and D. Breuer (2013), Thermo-chemical evolution of Mercury's interior, *J. Geophys. Res. Planets*, *118*, 2474–2487, doi:10.1002/jgre.20168.

Watters, T. R., et al. (2012), Tectonic features of Mercury: An orbital view with MESSENGER, presented at 43rd Lunar Planet. Sci. Conf., abstract 2121, pp. 16–17. [Available at http://www.lpi.usra.edu/meetings/lpsc2012/pdf/2121.pdf.]

Wetherill, G. W. (1988), Accumulation of Mercury from planetesimals, in *Mercury*, edited by F. Vilas, C. R. Chapman, and M. Matthews, pp. 670–691, Univ. of Ariz. Press, Tucson, Ariz.

Whitford-Stark, J. L., and J. W. Head (2000), Stratigraphy of Oceanus Procellarum basalts: Sources and styles of emplacement, *J. Geophys. Res.*, *85*(B11), 6579–6609, doi:10.1029/JB085iB11p06579.

Wilson, L., and J. W. Head (1981), Ascent and eruption of basaltic magma on the Earth and Moon, *J. Geophys. Res.*, *86*(B4), 2971–3001, doi:10.1029/JB086iB04p02971.

Xiao, Z., R. G. Strom, C. R. Chapman, J. W. Head, C. Klimczak, L. R. Ostrach, J. Helbert, and P. D'Incecco (2014), Comparisons of fresh complex impact craters on Mercury and the Moon: Implications for controlling factors in impact excavation processes, *Icarus*, *228*, 260–275, doi:10.1016/j.icarus.2013.10.002.

Ziethe, R., K. Seiferlin, and H. Hiesinger (2009), Duration and extent of lunar volcanism: Comparison of 3D convection models to mare basalt ages, *Planet. Space Sci.*, *57*(7), 784–796, doi:10.1016/j.pss.2009.02.002.